Revista Hábitat Sustentable Vol. 11, N°. 2. ISSN 0719 - 0700 / Págs. 60 - 71
https://doi.org/10.22320/07190700.2021.11.02.05

Recibido 19/08/2021
Aceptado 15/12/2021

THERMAL AND LIGHTING EVALUATION IN LIGHT ROOF PROTOTYPES, FOR HOT HUMID CLIMATES

EVALUACIÓN TÉRMICA Y LUMÍNICA EN PROTOTIPOS DE CUBIERTAS LIGERAS, PARA CLIMA CÁLIDO HÚMEDO

EDISON BOLIVAR ORTIZ-ZAMBRANO
Ingeniero Civil
Estudiante de posgrado de la Maestría Académica con Trayectoria Profesional en Ingeniería Civil: Mención en Construcción de Vivienda Social, Instituto de Posgrado
Universidad Técnica de Manabí, Portoviejo, Ecuador
https://orcid.org/0000-0001-8858-1361
bolivar_ortiz@live.com

JEFFERSON TORRES-QUEZADA
Doctor en Arquitectrura, Energía y Medio Ambiente
Docente-Investigador
Universidad Católica de Cuenca
Cuenca, Ecuador
https://orcid.org/0000-0002-1832-1369
jefferson.torres@ucacue.edu.ec

JOSÉ FABIÁN VÉLIZ-PÁRRAGA
Doctor en Ciencias Técnicas
Docente Universidad Técnica de Manabí
Portoviejo, Ecuador
https://orcid.org/0000-0001-5356-4537
jfveliz@hotmail.com

RESUMEN

El techo de chapa de zinc es uno de los elementos más populares en la arquitectura latinoamericana, y en muchas otras regiones con climas cálido húmedo. Crear alternativas lumínicas y térmicas enfocadas en esta tipología implicaría profundos beneficios en el campo ambiental y social. El presente estudio, realizado en Manabí-Ecuador, evalúa tres prototipos de cubiertas ligeras, combinando el material Zinc con el PVC, con el fin de determinar la correcta configuración del material translucido para crear ambientes que estén dentro de los parámetros térmicos y lumínicos. Los resultados indican que el modelo de soluciones empíricas presenta la menor variación de temperatura interior, con un 32,63%, a diferencia de los 32,97% del modelo tipo cruz y de los 34,40% del modelo de franjas laterales. Adicionalmente, se evidenció que la mayor influencia de radiación solar sobre la cubierta se registra desde las 13:00 h hasta las 14:00 h aproximadamente.

Palabras clave
Ecuador, vivienda, techos, comportamiento térmico interior

ABSTRACT

The zinc sheet roof is one of the most popular elements in Latin American architecture, and in many other regions with warm humid climates. Creating lighting and thermal alternatives focused on this typology would imply major benefits in the environmental and social fields. This study carried out in Manabí, Ecuador, evaluates three prototypes of light roofs, combining zinc with PVC, in order to determine the correct configuration of translucent material to create environments that are within thermal and lighting parameters. The results indicate that the empirical solutions model has the lowest variation in indoor temperature, with 32.63%, unlike the 32.97% of the cross-type model, and the 34.40% of the side strip model. Additionally, it was seen that the greatest influence of solar radiation on the roof is recorded from 1:00 p.m. to 2 p.m. approximately.

Keywords
Ecuador, housing, roofs, indoor thermal behavior.

Revista Hábitat Sustentable Vol. 11, N°. 2. ISSN 0719 - 0700 / Págs. 60 - 71
https://doi.org/10.22320/07190700.2021.11.02.05

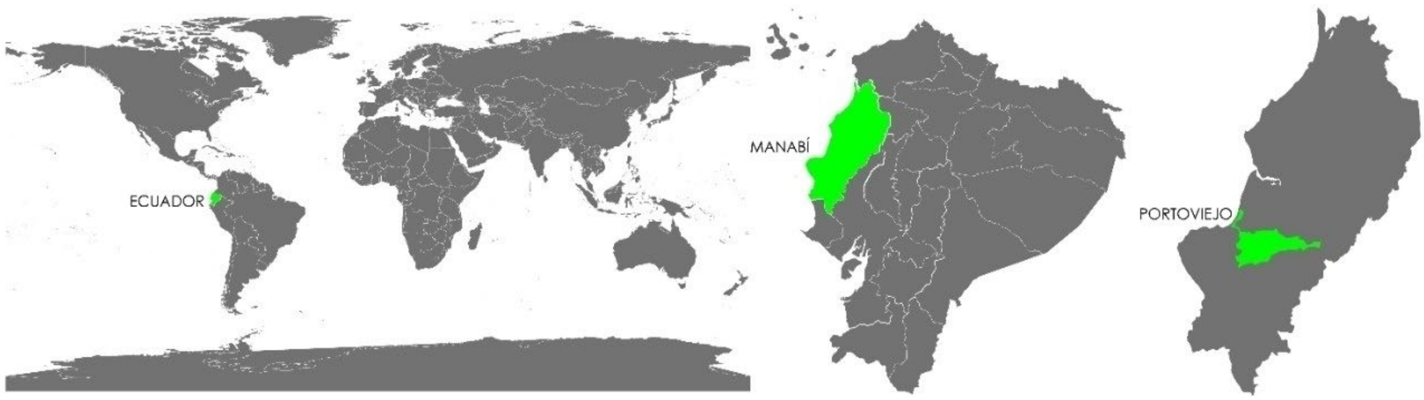

Figure 1. Geographic location of the study area. Source: Prepared by the authors.

INTRODUCTION

The roof is the top part of a building, whose main function is protecting the inside from the weather and external threats. This structural element is classified by its shape, material, and complexity (Hernández-Salomón, Rizo-Aguilera & Frómeta-Salas, 2017). One of the multiple options on the Ecuadorian market, and the most commonly used in the construction of social housing (SH), is the metal roof, characterized on being a corrugated steel sheet coated in zinc and aluminum, known as *Aluzinc* (Véliz-Parraga & González-Couret, 2019). This roof typology stands out as an economic and resistant solution, that is easy to apply and has a good visual appearance. However, due to its simple structural form and low thermal transmittance, it does not provide optimal insulation conditions, which causes a fast passing of the heat flow in buildings, generating uncomfortable indoor environments (Rodríguez, 2017). On certain occasions, a translucent polyvinylchloride (PVC) tile, a salt (57%) and oil (43%) byproduct (plasticseurope, 2021), is used. However, its use is limited on having a high cost, and also because one of its characteristics is letting zenithal light through, which causes an increase in the calorific intensity within the dwelling. Zinc sheets, due to their chemical constitution, have a reflectance quality, which PVC sheets do not have. This feature of reflecting light is one of the most important ones, as it indicates the amount of solar radiant energy that a surface reflects. As such, this is a determining factor in the thermal behavior of roofs (Alchapar, Correa & Cantón, 2012). Likewise, this surface depends greatly on the position of the sun and, thus, on the geographical space where it interacts with the environment, which is due to the angle of inclination of the sunlight, that varies in latitude (0°-90° North and South) and longitude (0° - 180° East and West) of the Earth (Oster, 2021, p. 39). Regions close to latitude 0° have, as a condition, that the roof receives sunlight perpendicularly during the year. This is the case of Ecuador (Torres, Coch & Isalgué, 2019).

The aforementioned country is formed by 24 provinces. Bordering the Pacific Ocean, is the province of Manabí, and within this, the Portoviejo Canton (Figure 1). This province stands out on having annual average temperatures between 21°C and 29°C, divided into two climatic periods, dry and humid (Macías, 2018).

According to the National Meteorology and Hydrology Institute [INAMHI, in Spanish], for October 29th, 2020, at the end of the dry period, absolute maximum temperatures of 32°C were recorded (El Universo, 2020). For March 30th, 2018, the absolute maximum temperatures were 34.9°C (El Diario, 2018), and for July 10th, 2014, at the end of the humid period, absolute maximum temperatures of 35.5°C were reached (INAMHI, 2014). This retrospective longitudinal cutoff indicates the climatic phenomenon that occurs close to 0° latitude. In this context, it must be considered that the solar radiation received by the roof produces more than a third of the thermal gain inside a dwelling (Osuna-Motta, Herrera-Cáceres & López-Bernal, 2017) and that the housing solution typologies of the Portoviejo Canton, where low-rise buildings prevail (Couret & Párraga, 2019), have roofs predominantly made from steel sheets coated in zinc and aluminum (Véliz-Párraga & González-Couret, 2019). It is then clear that it is this construction element that is mainly responsible for the heat contributions inside dwellings.

PASSIVE ROOFING STRATEGIES

Regarding the thermal performance of roofs, different general aspects and strategies have been studied, such as location and orientation; increased loss through convection on using wind direction; shape factor or compactness; useful surface; and total volume of the thermal envelope and the thermal mass of its components (Sisternes, 2019).

All these strategies have been applied to reduce user thermal discomfort without needing to use active systems. Other measures use passive design techniques, focusing on heat reduction or gain through the roof (Torres, Viñachi, Cusquillo, Pazmiñon & Segarra, 2019). The most commonly used ones included: thermal insulation paints, green roofs (Garnica, 2020), and masking through solar protections like trees, buildings, slats, double skins (Rojas, Soto & Díaz, 2020; Balter, Ganem & Discoli, 2016). However, from all this range of strategies focused on solving the comfort of spaces, most only focus on giving a solution to thermal comfort, leaving aside lighting issues. This contrariety has been growing starting from the first industrial revolution (1760-1840), as an effect of technological transformations (Belén & López, 2016), on prioritizing the search for traditional energy alternatives, from the Roman ships that carried wood, to the exploitation of oil wells. Now, as is well-known, fossil fuel supplies will run out, while the sun will continue heating future generations (Izzo, 2017). From this arises the importance of studying solar energy capture.

SOLAR ENERGY: SHAPE AND CAPTURE

The sun is the main axis in the evolution of life on Earth, as it provides suitable conditions for the existence of living beings. This star is involved in all production cycles, and it even determines our progressive activities by the use of time. For this reason, human beings have needed to use and take advantage of the sun to be able to coexist with the environment: as a defense against the cold; to define harvesting times; and even as a promoter of vitamin D (Yépez, 2018). Nowadays, however, our actions are no longer ruled by the sun. Today, artificial light allows the permanent lighting of spaces inside the dwelling, which has caused changes in the biological clock, circadian cycles, eating, working, and resting times; disorders that are also considered agents of the obesity epidemic that society is facing (Iluminet, 2015).

Since the first urban regulations in ancient Greece, in the city of Olynthus, an urban-logic fabric was designed, oriented from east to west, to organize strips and facades so that dwellings would face the south, to guarantee solar access, and to improve the quality of the habitat. It is important to highlight the Hadrian Pantheon in Rome, from 126 AD, as due to its almost perfect orientation of five degrees N-NW, it exposes its entire architectural shape, linked intimately to sunlight, which causes a game of lights and shadows which, for many historians, marked a new indoor spatial conception (Linares, 2015).

Today, there are regulations and ordinances adapted to the needs of each nation about the right to solar access or the continuous availability of unobstructed direct sunlight (Contardo, Cecchi & Lara, 2017).

In international-scale research, done in 10 countries and 34 case studies, about the influence of solar energy on urban planning, it was determined that the selection of technology and the social acceptance of the types of materials play a key role when it comes to designing new urban fabrics, where the basis of environmental impact, the local economy, and the market offer, is found. It was concluded that the formal functional characteristics presented a pattern of straight edges and parallel stripes in the distribution of solar modules; the most suitable shape factor set up for solar energy protection and capture (Lobaccaro et al., 2019). Another study, focusing on the construction of a methodological guide to design economic passive solar buildings and reduce the use of heating, ventilation, and air-conditioning (HVAC) systems, analyzed the normal conditions of a building to then make modifications to its construction components (roof and envelope), to optimize the use of the micro-climate and evaluate the maximum temperature reached by the building during 24 hours of the day, as well as the factors that affect the indoor temperature (Marín, 2012). In research focused on verifying the use of solar energy in the Metropolitan Area of Mendoza, whose climatic conditions are similar to the object of this study, the close ties between urban morphology and solar access were determined: the shape factor, and the land occupation factor, are the agents that most determine urban regulation. From this it is inferred, that the greater the urban density, the lower the solar energy availability there is (Cárdenas & Vásquez, 2017).

One of the core concepts of bioclimatic architecture is the solar approach, which forces further planning of openings, which are responsible for the heat-light contribution (Monroy, 2006) and, on certain occasions, building ventilation, an aspect that, of course, increases the comfort sensation of the user, without needing to turn to the use of HVAC systems. As for lighting, to reach comfort standards, certain design criteria mentioned in the technical guidelines must be met, among which taking advantage of daylight in the lighting of IDAE (2005) buildings stands out: "the choice of the place, orientation, shape, and dimensions of the building, utilizing the contribution of overhead light" (p. 36). For this reason, designing buildings that consider the use of overhead light as a key source of lighting, leads to major benefits for users, from the regulation of melatonin production, to visual comfort (Ramírez & Orozco, 2015), to important energy savings (Villalba, Pattini & Córica, 2012). Therefore, the question arises:

If light roof prototypes are designed, combining zinc with PVC, will the level of lighting and thermal comfort rise? To answer the query, prototypes were built with materials from the new vernacular era for areas with warm climates, under the parameters of sustainability and environmental protection. It is sought that these work as a theoretical base for a roof design that is capable of allowing sunlight to pass through with a lower heat contribution, thus contributing towards improving the livability and quality of social housing.

METHODOLOGY

This study was carried out using an experimental approach, with a descriptive scope, and is inserted within the line of research of indoor comfort of the dwelling. It was carried out in the central region of the Ecuadorian coast, in the city of Portoviejo, between the coordinates S1°3'16.49" W80°27'16.02" (Antipodas, 2020). The experimentation was done between January and March 2021, when the maximum temperature was 29°C, and the minimum 23°C, the cloudiness was above 75%, daylight hours were constant, with a value of 12 hours and 9 minutes, and with a westerly wind direction (Table 1). The study was divided into 2 stages.

STAGE 1 (FIELD STUDY)

In the first methodological stage, the structured observation technique was used, where the building characteristics of the geographic setting were revealed (Canton of Portoviejo), and the study was limited to shed-roof dwellings with Aluzinc roofs. A sample of 308 housing solutions of the urban area, and 89 dwellings from the rural area, were analyzed. This analysis showed that, in the urban area, the use of translucent material on the roofs (RTM) represented 7.8% of the sample and, in the rural area, 5.6%; which together total 29 dwellings from the 397 analyzed.

The Canton of Portoviejo is formed by 9 urban and 7 rural parishes (Figure 2), where there are 70,428 dwellings, 51,851 of which are located in the urban area, and 18,577 in the rural area. Of these, 48,744 have an Aluzinc sheet roofing material: 37,855 in the urban area, and 10.889 in the rural area (Table 2) (National Institute of Statistics and Censuses [INEC, in Spanish], 2010).

FORMULA TO CALCULATE THE SAMPLE

To calculate the part of the global total which had the characteristics of the population, the probabilistic formula set out by Flores (2014) was used. This is indicated in equation 1:

Agents / Months	January	February	March
Temperature	Maximum of 29°C and Minimum of 23°C		
Cloudiness	75%-81% cloudy or mainly cloudy 75%-81%		
Rainfall	24%-54%	55%-60%	60%-40%
Daylight	12 hours 9 min.		
Humidity	93%-99%	99%-100%	100% Kte
Wind speed	14.2 to 11.8 km/h	11.7 to 10.3 km/h	10.1 km/h Kte
Wind direction	West 76%	West 76%	West 75%
Short wave radiation	5.6 kWh visible light and ultraviolet radiation.		

Table 1. External climatological factors. Source: Prepared by the authors.

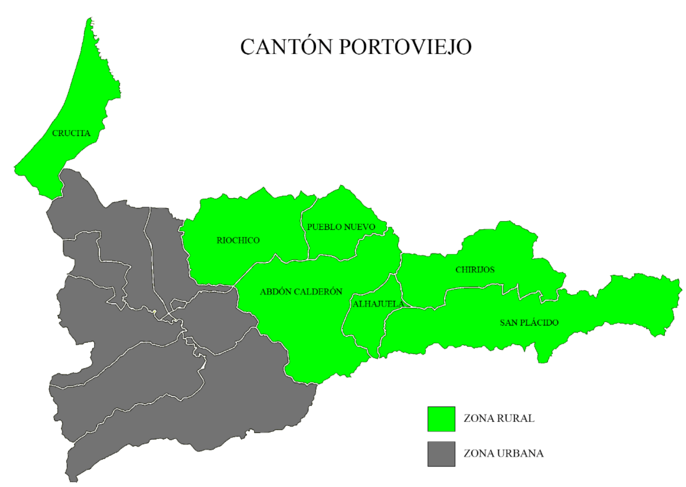

Figure 2. Map of the Canton of Portoviejo.
Source: Prepared by the authors.

$$n = \frac{PQ * N}{(N-1)\frac{E^2}{K^2} + PQ} \qquad (1)$$

Where:

n: Is the size of the probabilistic sample whose value is sought.
N: Is the size of the total population.
PQ: Is a constant of 0.25 of the population variance.
E: Is the maximum admissible error, that varies between 0.01 and 0.09
K: Is the correction coefficient of the error, which is a constant equal to 2.
(N-1): Is a relative constant for samples greater than 30 (Flores, p. 120-121).

Revista Hábitat Sustentable Vol. 11, N°. 2. ISSN 0719 - 0700 / Págs. 60 - 71
https://doi.org/10.22320/07190700.2021.11.02.05

CALCULATION OF THE SAMPLE SIZE OF THE PARISHES.

To define the number of parishes to be studied an admissible error of 1.16% of the 16 parishes was used, which resulted in 100% of these, as can be seen in equation 2.

$$n = \frac{PQ * N}{\frac{E^2}{K^2} + PQ} = \frac{0.25 * 16}{\frac{0.016^2}{2^2} + 0.25} = \frac{4}{0.25} = 16. \quad (2)$$

CALCULATION OF THE SAMPLE SIZE BY AREA.

Area	Order	Zinc roof (frequency)
Urban	9	37.855
Rural	7	10.889
Total	16	48.744

Table 2. Number of dwellings by area. Source: Prepared by the authors.

To calculate the number of housing solutions to be assessed, an admissible error of 5% of the 48,744 dwellings was used, which resulted in 397 dwellings (see equation 3). After this, the sample was calculated by share, for the different areas (see Table 3), and a stratified sample was made for the rural area (Table 4), given the geographic spread of this area. To end this first stage, the areas, frequency, sample size, and the RTM were described (Table 5).

$$n = \frac{PQ * N}{(N-1)\frac{E^2}{K^2} + PQ} = \frac{0.25 * 48.744}{(48.744 - 1)\frac{0.05^2}{2^2} + 0.25} = \frac{12.186}{30.71} = 397. \quad (3)$$

Area	Orden	Frequency	%	Cm
Urban	9	37.855	77.66	308
Rural	7	10.889	22.34	89
Total	16	48.744	100	397

Table 3. Number of dwellings to be assessed, by areas. Source: Prepared by the authors.

Rural Area	Orden	Frequency	%	Cm	Mtc
Abdón C.	1	3.104	28.51	25	2
Alhajuela	1	807	7.41	7	0
Chirijos	1	433	3.98	4	1
Crucita	1	1.812	16.64	15	0
Pueblo N.	1	658	6.04	5	1
Riochico	1	2.626	24.12	21	1
San Plácido	1	1.449	13.31	12	0
Total	7	10.889	100	89	5

Table 4. Stratification of the rural area. Source: Prepared by the authors.

Area	Orden	Frequency	%	Cm	Mtc
Urban	9	37.855	77.66	308	24
Rural	7	10.889	22.34	89	5
Total	16	48.744	100	397	29

Table 5. Number of dwellings that use a translucent material in the different areas of the Canton of Portoviejo.
Source: Prepared by the authors.

STAGE 2 (PROBE DESIGN AND ROOF MODELS)

To evaluate the thermal and lighting conditions through the experimental study, 4 model prototypes were built, with 1m x 1m x 1m dimensions, and plywood walls. The variables analyzed were the lighting and temperature characteristics inside the prototypes. The first model (A) is a base model, with a 100% metal roof, and it served to evaluate the environmental conditions and to compare them with the other three prototypes. Model (B) was designed based on the empirical overhead lighting solutions of the 29 dwellings observed, which opted to include PVC-based translucent material on the central upper part of their homes, where PVC represented 2% of the roof element. Model (C) was made from PVC and represented 10% of the total roof (two central strips of 5%, one horizontal and another perpendicular to the solar path), forming a cross on the center of the roof. Model (D) was designed based on recommendations of the IDAE technical guidelines and the overhead lighting methods of the 29 dwellings observed, which opted to include PVC-based translucent material on the outer lateral part of their dwellings (garages, pergolas), where PVC was 16% of the roof, represented in two 8% lateral strips, placed horizontally regarding the solar path. The prototypes were oriented on the East-West axis, with the highest part of the roof facing West, with a 10% slope, and they were positioned equidistant on the North-South axis, with a 1 m separation between them. The parameters measured in these were the indoor air temperature (Tai) and the indoor lighting level (E), for which HTC-2 digital thermo-hygrometers were used, and 2 digital apps: lux light meter Doogo apps and Luxometro: Smart Lux Meter.

RESULTS AND DISCUSSION

ANALYSIS OF PROTOTYPES A & B

The data collection of prototypes A and B was recorded for 15 days in January 2021, in 3 different periods (1-7, 10-14, 29-31), from 8 am to 6 pm, in 60-minute intervals. Figure 3 shows the average results of all the measurements taken at each one

Revista Hábitat Sustentable Vol. 11, N°. 2. ISSN 0719 - 0700 / Págs. 60 - 71
https://doi.org/10.22320/07190700.2021.11.02.05

horas	Tai/°C		E/Lux	
	A	B	A	B
8:00	25,76	25,92	0	45,0
9:00	26,07	26,14	0	45,9
10:00	27,38	27,72	0	53,6
11:00	29,85	30,05	0	53,9
12:00	30,78	30,98	0	54,1
13:00	32,23	33,93	0	54,5
14:00	32,45	34,16	0	54,5
15:00	32,27	33,97	0	54,5
16:00	32,09	33,86	0	54,1
17:00	30,15	30,35	0	50,7
18:00	29,19	29,38	0	42,3

Figure 3. Comparative matrix between prototype A and B.Source: Prepared by the authors.

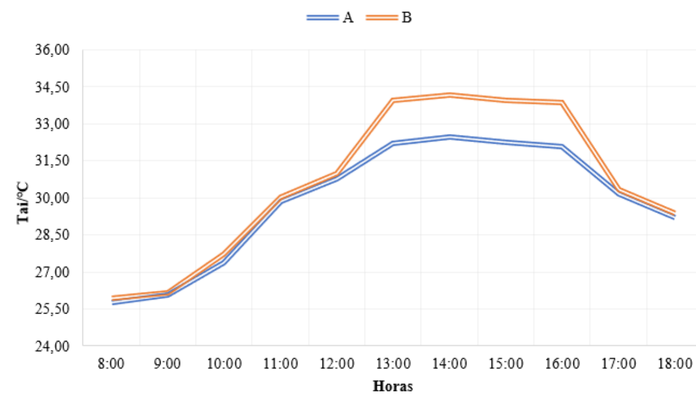

Figure 4. Comparative curves of the indoor temperature between the base model A and prototype B. Source: Prepared by the authors.

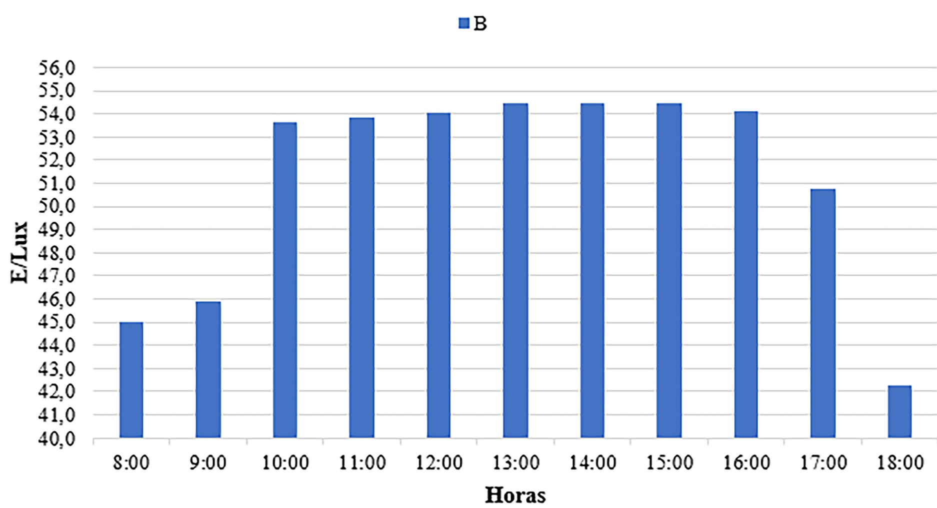

Figure 5. Indoor lighting levels of base model A and prototype B. Source: Prepared by the authors.

of the measurement times, and the structure of the A and B prototypes.

According to the results obtained from the base model A and prototype B, the average daily difference of indoor temperature between them is 0.75°C. The maximum temperature of model B is 34.16°C, recorded around 2 pm, which is 1.71°C higher than the indoor temperature of model (A). The maximum indoor temperature difference at 4 pm was 1.77°C (Figure 4). On the other hand, it was determined that the maximum lux value of prototype B was 54.5 lux, from 1 pm to 3 pm, approximately, and for model (A), the base model, this had a value of 0 lux (Figure 5).

ANALYSIS OF PROTOTYPES A & C

The data collection of prototypes A and C was made for 15 days in February 2021, during 3 periods (5-14, 19-21, 26-28), from 8 am to 6 pm, in 60-minute intervals. Figure 6 shows the average results of all the measurements taken in each one of the measurement times, as well as the structure of prototypes A and C.

Following the results obtained in the base model (A) and prototype C, the average daily indoor temperature difference between them is 1.25°C. The maximum temperature of model C is 36.57°C around 2 pm, which is 4.53°C higher than the indoor temperature of model (A) (Figure 7). Likewise, it was

horas	Tai/°C		E/Lux	
	A	C	A	C
8:00	25,72	25,88	0	64,6
9:00	26,16	26,32	0	67,6
10:00	27,47	28,39	0	69,9
11:00	29,95	30,15	0	70,5
12:00	30,85	31,13	0	70,5
13:00	31,96	34,35	0	71,3
14:00	32,04	36,57	0	71,2
15:00	31,77	34,18	0	70,8
16:00	31,74	33,47	0	69,7
17:00	29,91	30,26	0	69,5
18:00	28,69	29,26	0	57,9

Figure 6. Comparative matrix between prototypes A and C. Source: Prepared by the authors.

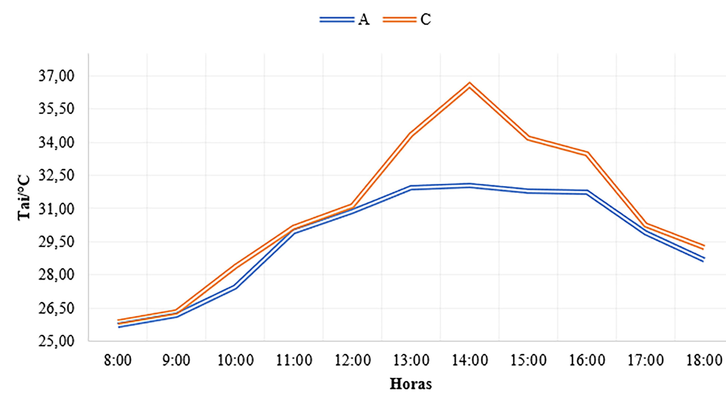

Figure 7. Comparative curves of the indoor temperature between the base model A and prototype C. Source: Prepared by the authors.

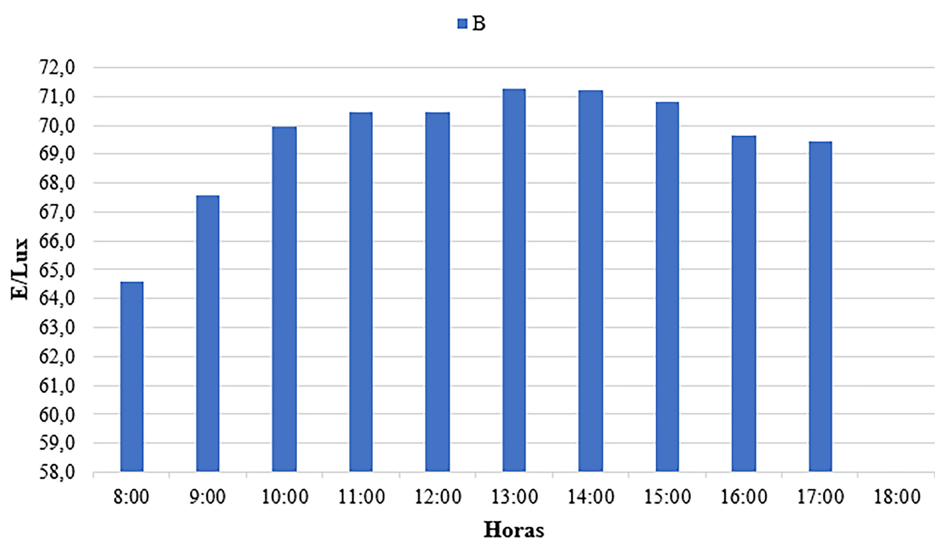

Figure 8. Indoor lighting levels of base model A and prototype C. Source: Prepared by the authors.

determined that the maximum lux value of prototype C was 71.3 lux, at 1 pm approximately, and for model (A), the base model, this had a value of 0 lux (Figure 8).

CALCULATION OF THE VARIATIONS OF PROTOTYPES A & D

The data collection of prototypes A and D was done for 15 days in March 2021, in 2 different periods (6-12, 19-26), from 8 am to 6 pm, in 60-minute intervals. In Figure 9, the average results of all the measurements taken in each one of the measurement times, and the structure of prototypes A and D, can be seen.

According to the results obtained from the comparison between the base model (A) and prototype D, the average daily indoor temperature difference is 1.90°C. The maximum temperature of model D is 38.26°C, recorded around 1 pm, which is 5.07°C higher than the indoor temperature of model (A) (Figure 10). It was also determined that the maximum lux value of prototype D was 118.4 lux, at approximately 1 pm, and that model (A), the base model, had a value of 0 lux (Figure 11).

COMPARISON OF THE DESIGN ALTERNATIVES

Under the analysis of this context, it was determined that, from 1 pm to 2 pm, approximately, there is a greater influence of solar radiation on the roof element, a result that matches Salgado (2012), whose research determined that, under normal conditions, the interphase from midday necessary for those

horas	Tai/°C		E/Lux	
	A	D	A	D
8:00	25,89	26,05	0	87,4
9:00	26,43	26,59	0	90,3
10:00	28,47	30,66	0	101,7
11:00	30,46	32,25	0	103,3
12:00	31,89	35,85	0	109,3
13:00	33,19	38,26	0	118,4
14:00	34,47	37,73	0	114,3
15:00	32,17	34,45	0	114,2
16:00	31,71	33,47	0	109,7
17:00	30,01	30,27	0	104,1
18:00	28,75	29,12	0	83,2

Figure 9: Comparative matrix between sheets A and D. Source: Prepared by the authors.

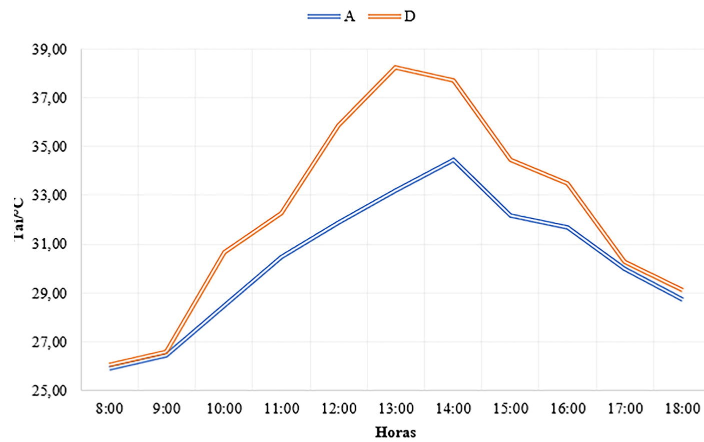

Figure 10. Comparative curves of the indoor temperature between base model A and prototype D. Source: Prepared by the authors.

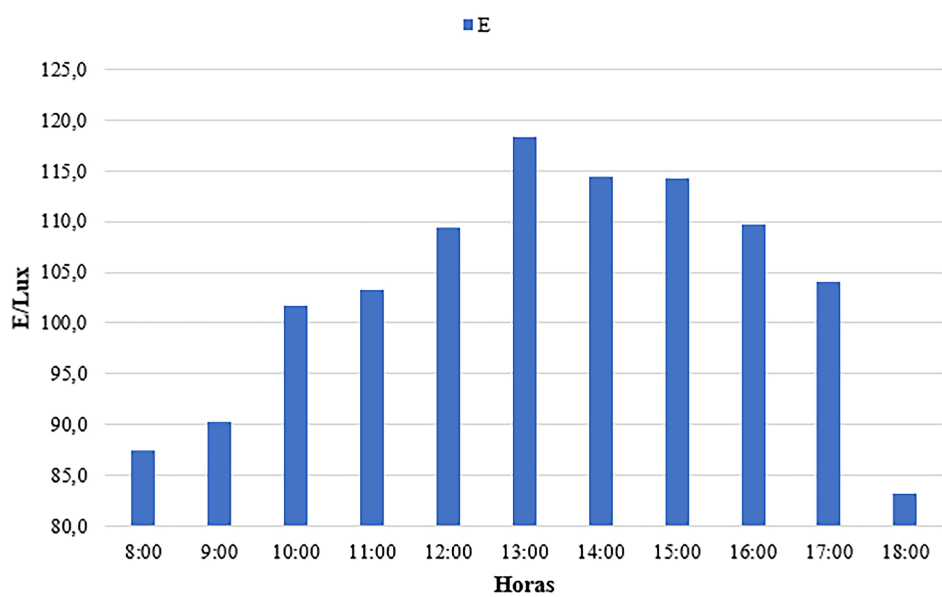

Figure 11. Indoor lighting levels of base model A and prototype D. Source: Prepared by the authors.

buildings to reach their maximum temperature was of 1 hour, 34 minutes and 10 seconds. Based on this study, the following stand out: Model B has the lowest indoor temperature variation, with 32.63%, which contrasts the 32.97% and 34.40% of models C and D, respectively. However, from the moment where the models reach the maximum temperature, model D has drastic temperature drops, reaching a relative balance at 3:30 pm, approximately (Figure 12), compared to the other prototypes. In addition, this model has values that exceed 100 lux from 10 am to 5 pm (Figure 13). This phenomenon is due to the amount of RTM (16%) with which it was designed, a percentage that exceeds the 10% recommended by IDAE (2005, p. 48), and the criterion corroborated by Monroy (2006), who states that the design criteria set out for vertical windows can also be adapted for the design roof hollows (p. 80), specifying that the 1/10 ratio is satisfactory.

In qualitative terms, model C, strictly designed following the setup of the shape factor to the occupied area of 10%, and with a cross shape, does not have good indoor light distribution. The opposite occurs with model D, which does project a suitable light distribution indoors, on having two lateral strips and the peculiarity that the narrowest part forms a perpendicular with the solar path; a measurable and observable aspect that is similar to the spatial distribution of cities of ancient Greece, famous for an orientation that guaranteed continuous access to sunlight. This setup also agrees with Lobaccaro et al. (2019), who analyzed 34 case studies in 10 different countries, determining that, in functional

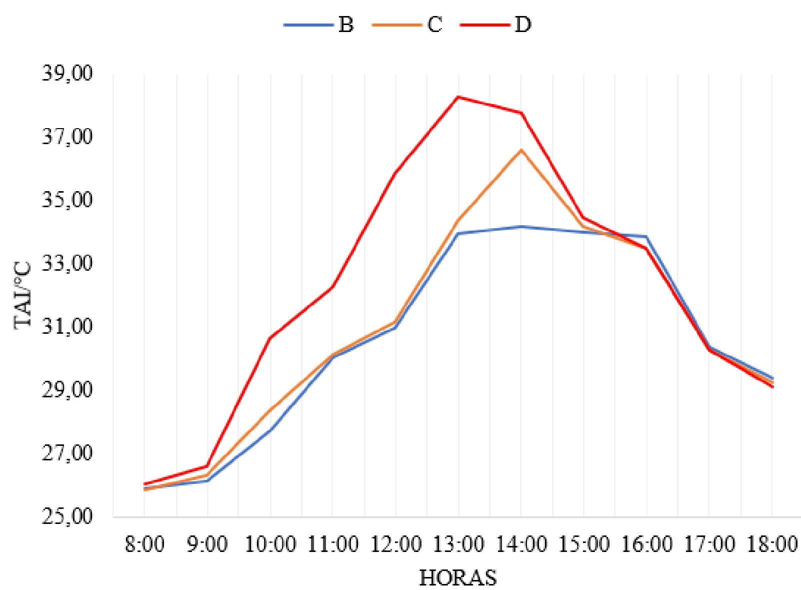

Figure 12. Indoor temperature of models B, C, and D.Source: Prepared by the authors.

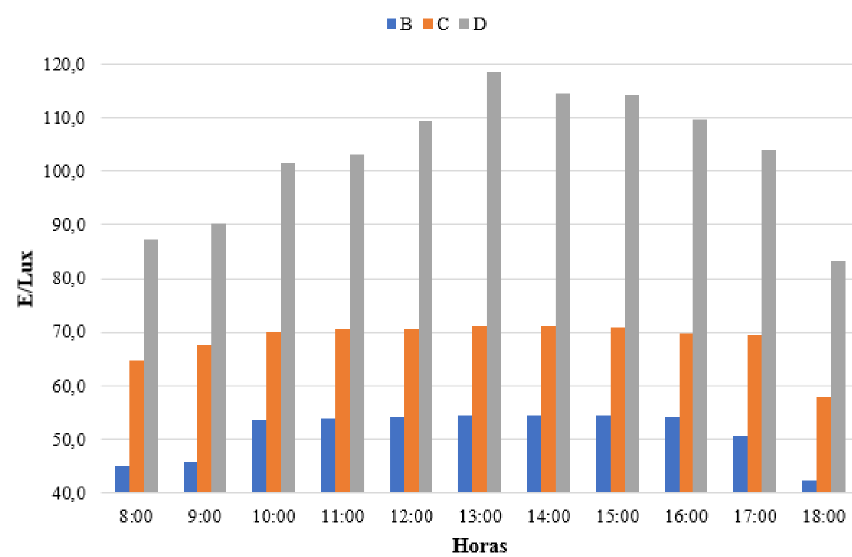

Figure 13. Indoor lighting levels of models B, C, and D. Source: Prepared by the authors.

terms of the shape factor, the distribution on straight edges for solar energy capture has better results. In summary, starting from the criteria mentioned and the experimentation done, this setup shows the best indoor light distribution, although for some authors, like Linares (2015), the play between light and shadow produced by other options will continue being a paradigm.

GENERAL CONSIDERATIONS

On being a developing country, Ecuador does not have regulations or municipal ordinances about the right to solar access, which can be seen in its urban fabric and, particularly, in the 397 housing solutions observed in this research, from which only 13.4% used translucent material on the roofs to capture overhead sunlight. Qualitatively, in the first stage of the study, as part of the systematic observation, in rural areas extremely hot dwellings were seen, with an absence of light, terraced on their side and rear walls, which added to crowding showed a low livability index. As for the needs of the area, the use of prototype D can be implemented. Likewise, it was possible to verify that the dominant roof material in the Canton is Aluzinc, which is even used as a double roof. Regarding the applicability of the prototypes, model B is recommended for specific overhead sunlight gains. Model C is not recommended, and model D, for dwellings that have some type of solar protection, and for terraced dwellings attached on their sides and rear.

CONCLUSION

In this work, three light roof prototype alternatives, with the combination of Zinc and PVC materials, were assessed, for warm climate areas under the parameters of sustainability and environmental protection. For this, passive overhead lighting capture strategies were used, such as orientation and the compacity of the shape factor, implementing the solar approach strategy, which would allow designing light roofs that improved the light contribution inside the dwelling, without generating spaces with overheating. The most important discovery of this methodological process, which was based on field measurements using scale models, was the determination of the time of greatest influence of the sun on the roof for this type of areas and the setup that must be given to the RTM, to design spaces that comply with suitable thermal and light characteristics to have healthy dwellings. One of the limitations of this research was the lux data collection, due to its high variability index in space-time.

This allows discarding the hypothesis set out, to a certain degree, as the incorporation of RTM on the roof increases the lighting level, but its shape factor setup does not reduce or maintain the temperature inside the tested models. Now, the results of model D have drastic temperature drops from the moment they reach their peak, and at the same time record a better indoor light distribution, that is to say, a better lux level. As a conclusion, it is important to mention that the question emerges about what would happen if these construction strategies were applied on double-skin roofs and gable roofs. Thus, as the next step to perfect the prototypes presented herein, this study recommends analyzing the incorporation of translucent material on gable roofs.

ACKNOWLEDGMENTS

The authors would like to thank the Technical University of Manabí and the Postgraduate Institute – UTM. Thanks are given to the research grant within the Master's Degree in Civil Engineering, with a Minor in Social Housing Construction: RPC-S=-10-No.130-2019. Thanks are given to the Catholic University of Cuenca, project DAMA-215543.

BIBLIOGRAPHICAL REFERENCES

Alchapar, N., Correa, E. y Cantón, M. (2012). Índice de reflectancia solar de revestimientos verticales: Potencial para la mitigación de la isla de calor urbana. *Ambiente Construido, 12*(3), 107-123. DOI: https://doi.org/10.1590/S1678-86212012000300008

Antipodas (2020). Coordenadas de Portoviejo (Ecuador). Recuperado de https://www.antipodas.net/coordenadaspais/ecuador/portoviejo.php

Balter, J., Ganem, C. y Discoli, C. (2016). Ahorros en los consumos para enfriamiento de espacios interiores mediante la evaluación de sistemas de protección solar en edificios residenciales en altura. El caso de la "ciudad-oasis" de Mendoza, Argentina. *Hábitat Sustentable*, *6*(1), 72-83. Recuperado de http://revistas.ubiobio.cl/index.php/RHS/article/view/2353

Belén, B. y López, J. (2016). *Revolución industrial*. Recuperado de https://economipedia.com/definiciones/primera-revolucion-industrial.html

Cárdenas, L. Y Vásquez, P. (2017). Potencial solar en fachadas integrando la densidad urbana: Una mirada crítica a la norma urbanística chilena. *AUS [Arquitectura / Urbanismo / Sustentabilidad], 18*, 58-63. DOI: https://doi.org/10.4206/aus.2015.n18-10

Contardo, J., Cecchi, C. y Lara, K. (2017). Acceso Solar: Un derecho urbano para la calidad de vida vulnerado desde la Gentrificación contemporánea. El caso de la comuna de Estación Central, Chile. *Revista 180*, *0*(39). DOI: http://dx.doi.org/10.32995/rev180.Num-39.(2017).art-283

Couret, D. y Párraga, J. (2019). Evolución de la vivienda de interés social en Portoviejo. *Cuadernos de Vivienda y Urbanismo*, *12*(23). DOI: https://doi.org/10.11144/Javeriana.cvu12-23.evis

El Diario (2018). Temperatura más alta en Portoviejo. *El Diario*. EDIASA. Recuperado de https://www.eldiario.ec/noticias-manabi-ecuador/467707-temperatura-mas-alta-en-portoviejo/

El Universo (2020). Se registran altas temperaturas en Guayas y Manabí, este es el pronóstico para el viernes 30 de octubre. *El Universo*. Recuperado de https://www.eluniverso.com/noticias/2020/10/29/nota/8031442/inamhi-pronostico-tiempo-ecuador-30-octubre-ecuador-radiacion

Flores, C. (2014). *Introducción a la Estadística*. Manta: Mar Abierto.

Garnica, A. (2020). Efecto en la temperatura para mitigar la Isla de Calor utilizando dos ecotecnias. *Meio Ambiente (Brasil)*, *2*(5). Recuperado de http://www.meioambientebrasil.com.br/index.php/MABRA/article/view/92

Hernández-Salomón, M., Rizo-Aguilera, L. y Frómeta-Salas, Z. (2017). Recomendaciones de diseño con enfoque medioambiental para cubiertas ligeras en edificaciones del centro histórico de Santiago de Cuba. *Ciencia en su PC,* (1), 70-88. Recuperado de https://www.redalyc.org/articulo.oa?id=181351125006

IDAE (2005). *Guía técnica: Aprovechamiento de la luz natural en la iluminación de edificios*. Recuperado de https://www.idae.es/publicaciones/guia-tecnica-aprovechamiento-de-la-luz-natural-en-la-iluminacion-de-edificios

Iluminet (2015). El equilibrio entre luz artificial y natural puede ser una clave contra la obesidad. *Iluminet. Revista de iluminación*. Recuperado de https://www.iluminet.com/iluminacion-artificial-obesidad/

Instituto Nacional de Estadística y Censos [INEC] (2010). *Población y Demografía*. Recuperado de https://www.ecuadorencifras.gob.ec/censo-de-poblacion-y-vivienda/

Instituto Nacional de Meteorología e Hidrología [INAMHI] (2014). *Análisis Climatológicos*. Recuperado de http://www.serviciometeorologico.gob.ec/meteorologia/bolhist/cli/2014/MENSUAL/bol_jul_2014.pdf

Izzo, G. (2017). *Perspectiva de la energía nuclear en la futura matriz energética*. Tesis de magíster. Universidad Nacional de La Plata. DOI: https://doi.org/10.35537/10915/61231

Linares, T. (2015). Further observations on the light in the Pantheon in Rome. *VLC arquitectura. Research Journal*, *2*(1), 33-55. DOI: https://doi.org/10.4995/vlc.2015.3376

Lobaccaro, G., Croce, S., Lindkvist, C., Probst, M., Scognamiglio, A., Dahlberg, J., Lundgren, M. y Wall, M. (2019). A cross-country perspective on solar energy in urban planning: Lessons learned from international case studies. *Renewable and Sustainable Energy Reviews*, *108*, 209-237. DOI: https://doi.org/10.1016/j.rser.2019.03.041

Macías, A. (2018). Análisis de los Factores Endógenos y Exógenos Higrotérmicos del Sector los Bosques Cantón Portoviejo y Propuesta de Solución. Tesis de doctorado. Universidad laica "Eloy Alfaro" de Manabí. Recuperado de https://repositorio.uleam.edu.ec/handle/123456789/2330

Marín, F. (2012). Evaluación del rendimiento de calefacción o refrescamiento producido por los elementos constructivos y microclima de una vivienda pasiva. Una forma de integrar el rendimiento del confort térmico pasivo a su administración del ciclo de vida de un edificio. *Revista INVI*, *27*(75), 171-197. Recuperado de https://revistainvi.uchile.cl/index.php/INVI/article/view/62339/66418

Monroy, M. (2006). *Manuales de Diseño ICARO*. [Manual-1-ILUMINACION]. Recuperado de https://m2db.wordpress.com/2014/09/01/manuales-de-diseno-icaro/

Oster, L. (2021). *Astronomía moderna*. Recuperado de https://books.google.es/books?id=xpAXEAAAQBAJ&hl=es&source=gbs_navlinks_s

Osuna-Motta, I., Herrera-Cáceres, C. y López-Bernal, O. (2017). Techo plantado como dispositivo de climatización pasiva en el trópico. *Revista de Arquitectura (Bogotá)*, *19*(1), 42-55. DOI: https://doi.org/10.14718/RevArq.2017.19.1.1109

Plasticseurope (2021). *Tipos de plásticos*. Recuperado de https://www.plasticseurope.org/es/about-plastics/what-are-plastics/large-family

Ramírez, A. y Orozco, A. (2015). La envolvente arquitectónica y su influencia en la iluminación natural. *Hábitat Sustentable*, *5*(1), 44-53. Recuperado de http://revistas.ubiobio.cl/index.php/RHS/article/view/1811

Rodríguez, S. (2017). *Diseño y evaluación de un sistema de doble cubierta ventilada para reducir la transmisión de calor al interior de la vivienda media en Puerto Vallarta, Jalisco*. Tesis de maestría. Universidad Autónoma Metropolitana, México. Recuperado de http://zaloamati.azc.uam.mx/handle/11191/5944

Rojas, J., Soto, P. y Díaz, H. (2020). Evaluación dinámica de control solar lumínico. Propuestas en una biblioteca de arquitectura moderna en Santiago. *Estoa. Revista de la Facultad de Arquitectura y Urbanismo de la Universidad de Cuenca*, *9*(18), 125-137. DOI: https://doi.org/10.18537/est.v009.n018.a11

Sisternes, Á. (2019). Diseño pasivo: Concepto, ventajas y desventajas. *Kömmerling*. Recuperado de https://retokommerling.com/diseno-pasivo/

Torres, B., Viñachi, J., Cusquillo, J., Pazmiño, C. y Segarra, M. (2019). Aprovechamiento de la arquitectura pasiva para la reducción de carga térmica por ganancia solar en un edificio de la Facultad de Arquitectura de la Universidad de Guayaquil. *Extensionismo, Innovación y Transferencia Tecnológica*, *5*(0), 378-388. DOI: https://doi.org/10.30972/eitt.503775

Torres, J., Coch, H. y Isalgué, A. (2019). Assessment of the reflectivity and emissivity impact on light metal roofs thermal behaviour, in warm and humid climate. *Energy and Buildings*, *188-189*, 200-208. DOI: https://doi.org/10.1016/j.enbuild.2019.02.022

Véliz-Párraga, J. y González-Couret, D. (2019). Vivienda de interés social en Portoviejo. ambiente térmico interior. *AUS [Arquitectura / Urbanismo / Sustentabilidad]*, (26), 35-41. DOI: https://doi.org/10.4206/aus.2019.n26-07

Villalba, A., Pattini, A. y Córica, M. (2012). Análisis de las características morfológicas de las envolventes edilicias y del entorno urbano desde la perspectiva de la iluminación natural. *Ambiente Construido*, *12*(4), 159-175. DOI: https://doi.org/10.1590/S1678-86212012000400011

Yépez, K. (2018). 10 beneficios de tomar el sol para nuestra salud. *Elsevier Connect*. Recuperado de https://www.elsevier.com/es-es/connect/ciencia/beneficios-salud-del-sol